Journal of Chemical Health Risks

www.jchr.org

JCHR (2025) 15(6), 1753-1772 | ISSN:2251-6727

Liquid Crystal Schiff's base esters of Isoniazid with 4-*n* -Alkoxy benzoic acids derivatives: Antituberculosis Drug

[a]Keval bambhroliya, [b]Sanskruti Patel, [b]Prashant Trivedi, [c]Chetan Sangani, [d]Maitreyi Zaveri, [a]*Hemant Patel.

[a]Shree Maneklal M. Patel Institute of Sciences & Research Sector 15/23, Gandhinagar-382024, Kadi Sarva Vishwavidhyalaya, Gandhinagar, India

[b] Department of Chemistry, School of Sciences, Gujarat University-380007, Ahmedabad, India

[c]Department of Chemistry, Government Science College Gandhinagar-382016, Gujarat University, Gujarat, India

[d]Department of Pharmacognosy and Regulatory Affairs, K.B. Institute of Pharmaceutical Education and Research, A constituent college of Kadi Sarva Vishwavidyalaya

(Received: 05 October 2025 Revised: 15 November 2025 Accepted: 10 December 2025)

KEYWORDS

Isoniazid (INH), Antituberculosis Drug, Schiff's base method

ABSTRACT:

Isoniazid LC derivative is a synthetic antimicrobial and one of the most important first-line drugs used in the treatment of tuberculosis since 1952. One new mesogenic homologous series of isoniazid with Schiff's base ester having Alkyl 4-[(E)-{4-[(pyridin-4-ylcarbonyl)hydrazono]methyl}phenoxy]benzoate have been synthesized & molecular structures were characterized by the standard spectroscopic methods and elemental analysis. Isoniazid Schiff's base ester synthesized by condensing 4-n alkoxy benzoyloxy benzaldehyde [A] with isoniazid [B] by Schiff's base method [B] synthesized by condensing in the presence of an alcoholic acidic medium. All members in series is exhibiting nematic-mesophase..

Introduction

Tuberculosis (TB) is currently the most severe infectious illness, accounting for more deaths than the human immunodeficiency virus (HIV).**[1]** According to the World Health Organization's (WHO) most recent surveys, 1.3 million TB-related deaths and 10 million new cases worldwide.**[2]** Various cases were documented in Brazil, according to statistics from the National Health Department. **[3–4]** The basic chemical structure of isoniazid, frequently referred to as is nicotinic acid hydrazide (INH), is made up of a pyridine ring and a hydrazine group that is linked to the pyridine (N) nitrogen. 4-cyanopyridine and hydrazine hydrate activate in an aqueous alkaline environment at 100°C under reflux for 7 hours to yield isoniazid, which then crystallizes in ethanol and exhibits LC properties.**[5]** Synthesizing new crystalline forms of active pharmaceutical ingredients (APIs) and enhancing their liquid crystal characteristics. **[6–9]** Standard anti-TB therapy consists of multi-drug formulations that includes isoniazid (INH), rifampicin (RIF), ethambutol (EMB), and pyrazinamide (PZA) in combinations. It has been demonstrated that the formulation of anti-TB drugs as fixed-dose combinations (FDCs) improves patient comfort and reduces gastrointestinal (GIT) adverse effects **[10,11]**. Within two months of treatment, INH and RIF, the two most efficient anti-TB medications, eradicate about 99% of tubercular bacilli. INH & RIF are in combination in FDC pills. The duration of treatment can be prolonged by 18 to 6 months through the utilization of both-medications **[12,13]**. The synthetic novel homologous series of compounds' general structural formula is displayed in Scheme **1**.

Journal of Chemical Health Risks

www.jchr.org

JCHR (2025) 15(6), 1753-1772 | ISSN:2251-6727

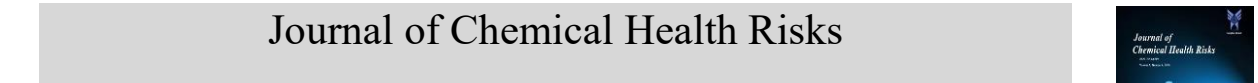

Graphical Abstract:

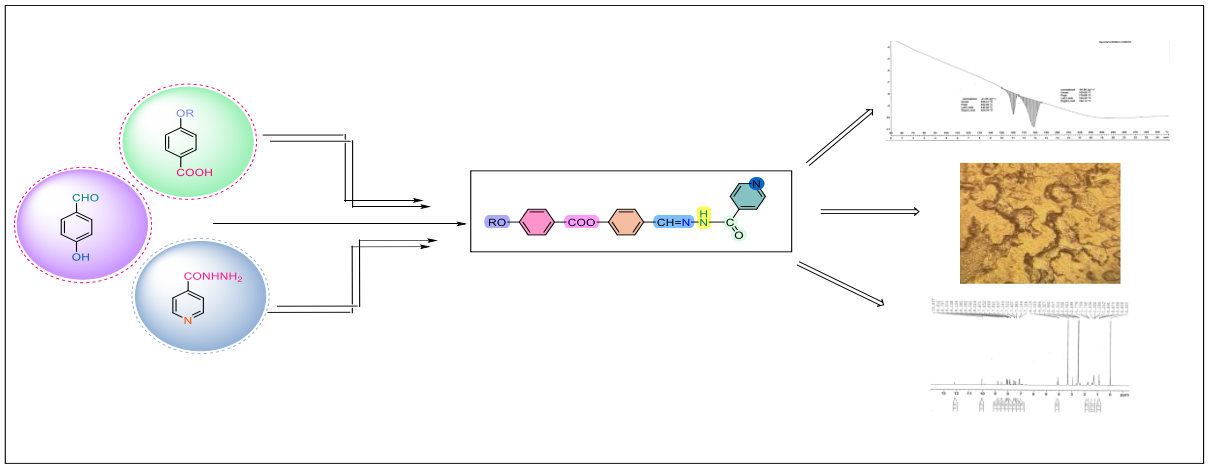

Synthetic Route:

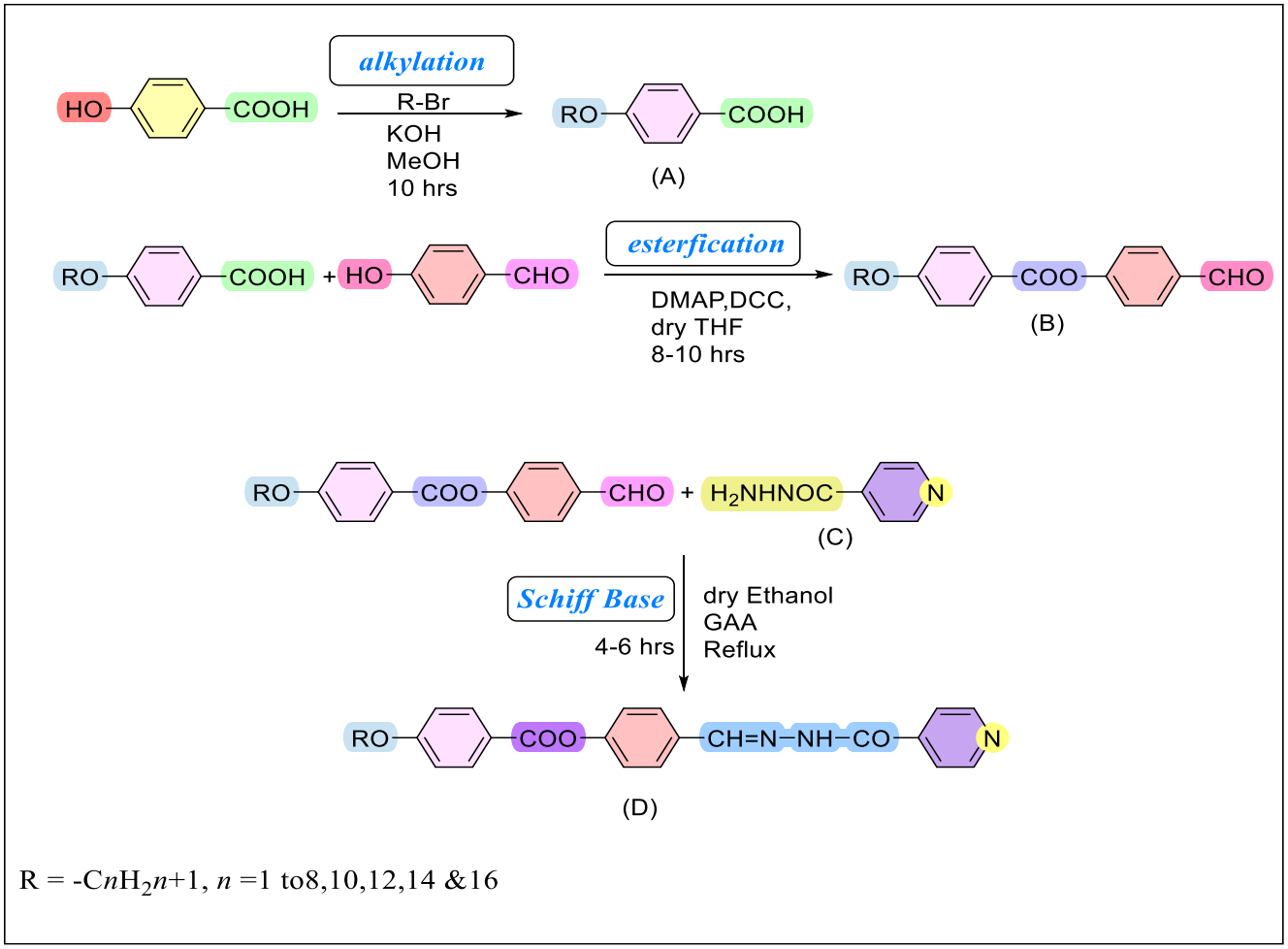

Scheme 1: Synthesize of compounds Series 1

Journal of Chemical Health Risks

www.jchr.org

JCHR (2025) 15(6), 1753-1772 | ISSN:2251-6727

Experimental

Synthesis

P-hydroxy benzoic acid, p- hydroxy benzaldehyde, *n*-alkyl halides, 1-bromoalkanes, isoniazide, DCC [dicyclohexyl carbodiimide], DMAP [dimethyl amino pyridine], potassium hydroxide, methanol, and ethanol were used exactly as supplied. Prior to usage, the solvents were distilled and dried. Using a Coleman carbon-hydrogen analyser, the compounds were microanalyzer, and the results closely match the calculated values. KBr pellets were used to determine the IR spectra using a Shimadzu IR-408 spectrophotometer. Tetramethyl silane (TMS) was used as the terminal reference standard in order to generate 1H NMR spectra using a Perkin-Elmer R-32 instrument. All of the compounds were dissolved in $CDCl_3$, and the chemical alterations are expressed as & (parts per million) downfield from the standard. Thermal polarized light microscopy was utilized to govern the phase assignments and transition temperatures utilizing a polarizing microscope (LeitzLaborlux 12 POL) with a heating stage. The enthalpies of transition, denoted by means of Jg^{-1}, were measured at a scanning rate of 10˚ C min-1 using a Mettler TA-4000 system. Pure indium served as the reference for calibrating the device.

Alkyl 4-[(E)-{4-[(pyridin-4-ylcarbonyl)hydrazono]methyl}phenoxy]benzoate

4-*n*-Alkoxybenzoic acids [**A**]:

Para-anisic acid, B. D. H., or para-methoxybenzoic acid, was employed. There are several recognized techniques for alkylating para-hydroxybenzoic acid **[14, 15]**

Nonetheless, Dave and Vora's **[16]** Methodology was used in this investigation. After dissolving 0.1 moles of para-hydroxybenzoic acid, 0.12 moles of suitable *n*-bromoalkane, and 0.25 moles of potassium hydroxide (KOH) in 100 milliliters of ethanol, the mixture was refluxed for seven to eight hours. After adding 25 milliliters of a 10% aqueous potassium hydroxide (aq. KOH) solution, reflux was maintained for two to three hours in order to hydrolyze any ester that might have developed. After being dissolved in 100 milliliters of ethanol, 0.1 moles of para-hydroxybenzoic acid, 0.12 moles of suitable n-bromoalkane, and 0.25 moles of potassium hydroxide (KOH) were refluxed for seven to eight hours. For two to three hours, reflux was maintained while 25 milliliters of a 10% aqueous potassium hydroxide (aq. KOH) solution was added in order to hydrolyze any ester that might have developed. 50% cold aqueous hydrochloric acid (HCl) was added to the solution after it had cooled, resulting in a white precipitate. A constant transition temperature was achieved by crystallizing the alkoxy [RO-] acids from methanol or acetic acid one or two times, depending on the higher member. There is a good agreement between the transition temps and the literature review.

Synthesis of 4-*n* alkoxy benzoyloxy benzaldehyde [B]

The process for creating involves 4-*n* alkoxy benzoyloxy benzaldehyde **[B]** dissolving 0.1 mole of p- hydroxy benzaldehyde in 50 milliliters of dry tetrahydrofuran (THF), adding the required 4-*n*-Alkoxybenzoic acids (0.1mole) and DMAP (0.1mole), and stirring at room temperature. Dropwise additions of DCC **[17]** (0.1mole) dissolved in 10 ml of dry tetrahydrofuran (THF) were made to the mixture, which was then constantly swirled for 12 hours at room temperature. Ultimately, the mixture was filtered, and slow evaporation was used to extract the solvent. The resulting yellow solid was recrystallized twice using ethanol, yielding the pure chemical. All of the compounds' purity was examined using thin-layer chromatography (Merck 60 F254) and seen under short-wave UV light.

Synthesis of Alkyl 4-[(E)-{4-[(pyridin-4-ylcarbonyl)hydrazono]methyl}phenoxy]benzoate [C]
In a 60 ml solution of dry ethanol (C_2H_5OH), isoniazid **[C]** (0.1mole) and 4-*n* alkoxy benzoyloxy benzaldehyde (0.1mole) were refluxed for three hours after a few drops of glacial acetic acid (CH_3COOH) were added. The filtrate was then allowed to evaporate in the fume hood at ambient temperature after the reaction mixture had been filtered. Before being employed in a subsequent procedure **[18]**

Journal of Chemical Health Risks

www.jchr.org

JCHR (2025) 15(6), 1753-1772 | ISSN:2251-6727

Table 1: **Phase transition temperatures (ºC) of series I compounds**

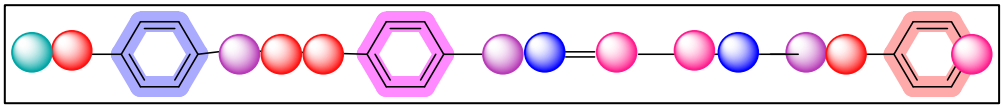

= Carbon, = Hydrogen, = Oxgyen, = Nitrogen, = R(alkyl group)

Compound No.	R= -C_nH_{2n+1} *n* =	Cr		N		I
1	*1*	•	200	•	222	•
2	*2*	•	185	•	221	•
3	*3*	•	133	•	219	•
4	*4*	•	160	•	178	•
5	*5*	•	137	•	209	•
6	*6*	•	135	•	205	•
7	*7*	•	131	•	201	•
8	*8*	•	118	•	199	•
9	*10*	•	122	•	185	•
10	*12*	•	158	•	178	•
11	*14*	•	136	•	166	•
12	*16*	•	108	•	154	•

Cr=crystalline solid; N=nematic phase; I=isotropic liquid phase; •=phase exists

Journal of Chemical Health Risks

www.jchr.org

JCHR (2025) 15(6), 1753-1772 | ISSN:2251-6727

Table 2: Elemental Analysis

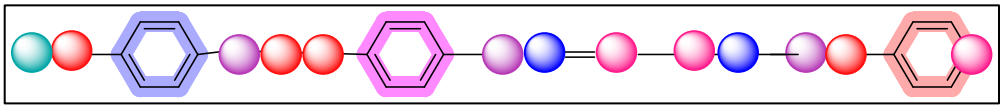

Compound No.	R C_nH_{2n+1} n=	Formula	% Required (% found) C	H	N
1	**1**	$C_{21}H_{17}O_4N_3$	67.19 (67.15)	4.56 (4.52)	11.19 (11.15)
2	**2**	$C_{22}H_{19}O_4N_3$	67.86 (67.84)	4.92 (4.95)	10.79(10.77)
3	**3**	$C_{23}H_{21}O_4N_3$	68.47 (68.48)	5.25 (5.27)	10.42 (10.45)
4	**4**	$C_{24}H_{23}O_4N_3$	69.05 (69.08)	5.55 (5.52)	10.07 (10.09)
5	**5**	$C_{25}H_{25}O_4N_3$	69.59 (69.57)	5.84 (5.83)	9.74 (9.77)
6	**6**	$C_{26}H_{27}O_4N_3$	70.07 (70.09)	6.11 (6.02)	9.43 (9.45)
7	**7**	$C_{27}H_{29}O_4N_3$	70.57 (70.59)	6.36 (6.34)	9.14 (9.12)
8	**8**	$C_{28}H_{31}O_4N_3$	71.02 (71.03)	6.60 (6.63)	8.87 (8.90)
9	**10**	$C_{30}H_{35}O_4N_3$	71.83 (71.85)	7.07 (7.04)	8.38 (8.40)
10	**12**	$C_{32}H_{39}O_4N_3$	72.56 (72.57)	7.42 (7.43)	7.93 (7.95)
11	**14**	$C_{34}H_{43}O_4N_3$	73.22 (73.25)	7.77 (7.99)	7.53 (7.52)
12	**16**	$C_{36}H_{47}O_4N_3$	73.81 (73.85)	8.09 (8.07)	7.17 (7.18)

Table **2** shows that the elemental analysis of every chemical in the series was deemed adequate. The spectrum data of series I's representative members, some derivatives of *n*-butyloxy, *n*-octyloxy, *n*-dodecyloxy and tetradecyloxy are provided below.

Table 3: Phase transition temperatures (°C), enthalpy change, entropy change and normalised entropy of the series by DSC and POM measurement.

Compound	Transition	Peak temp./°C	ΔH/Jmol^{-1}	ΔS/kJmol^{-1} K^{-1}
I	Cr-N	200.1	33.73	0.0000712
	N-I	222.5	11.78	0.0000237
III	Cr-N	132.99	26.71	0.000065
	N-I	219.9	29.16	0.0000591
IV	Cr-N	160.06 178.66	21.58 54.98	

Journal of Chemical Health Risks

www.jchr.org

JCHR (2025) 15(6), 1753-1772 | ISSN:2251-6727

	N-I			0.00004983
				0.0001217
		158.13	13.15	
XII	Cr-N	177.58	33.18	
	N-I			0.0000304
				0.0000736

Spectral Data:

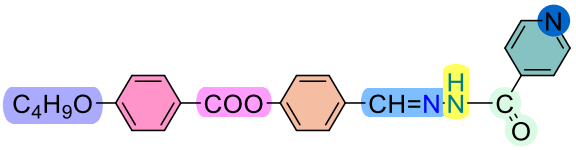

4-((2-isonicotinoylhydrazineylidene)methyl)phenyl 4-butoxybenzoate

Figure:1 IR Graph

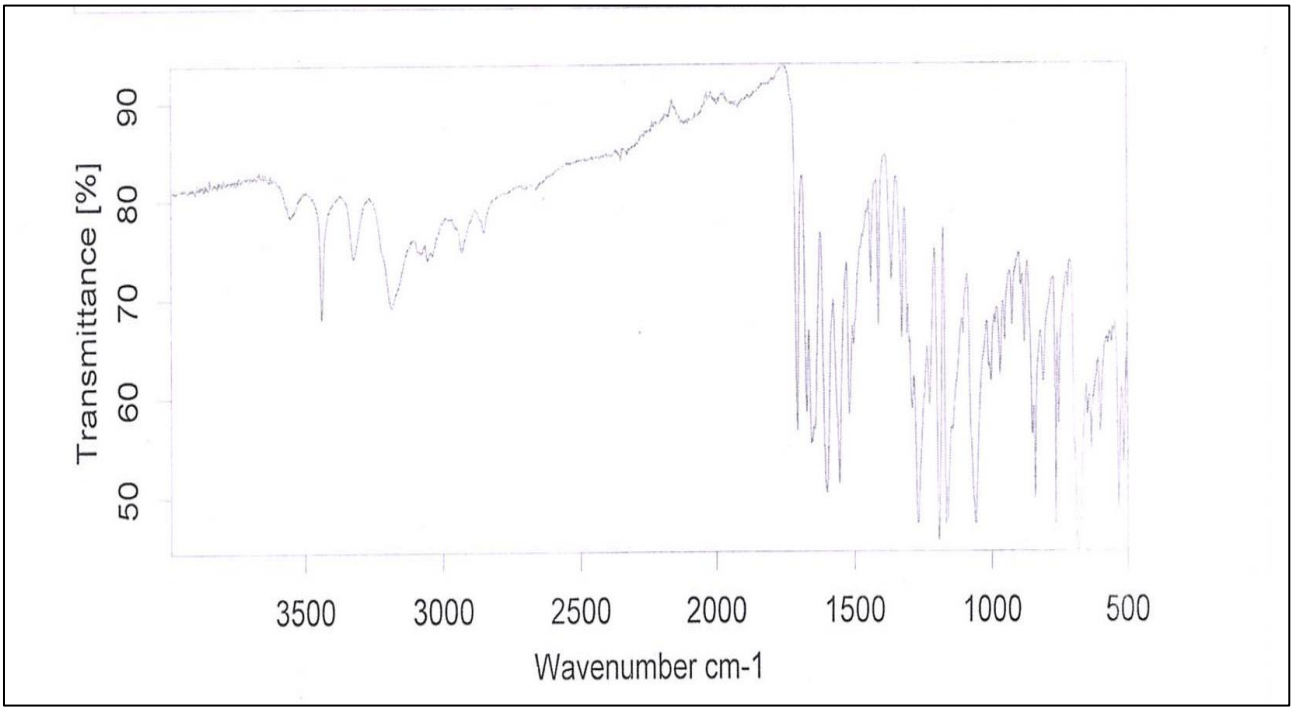

IR spectrum *(KBr)* ν_{max}/cm^{-1}**:** 3321(-NH-), 3054, 2927, 1703 (-COO-), 1653, 1597 (-HC=N-), 1552, 1364, 1291,1270, 839.
4-((2-isonicotinoylhydrazineylidene)methyl)phenyl 4-butoxybenzoate

Journal of Chemical Health Risks

www.jchr.org

JCHR (2025) 15(6), 1753-1772 | ISSN:2251-6727

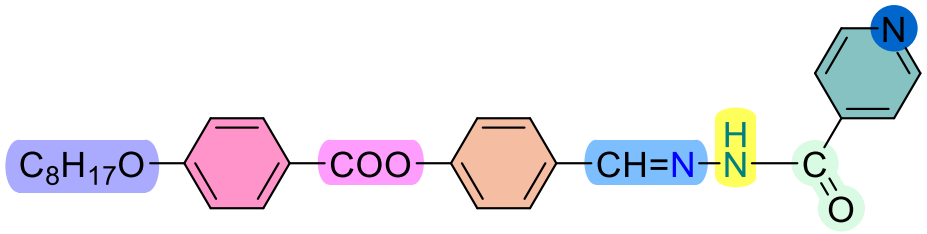

4-((2-isonicotinoylhydrazineylidene)methyl)phenyl 4-(octyloxy)benzoate

Figure:2 IR Graph

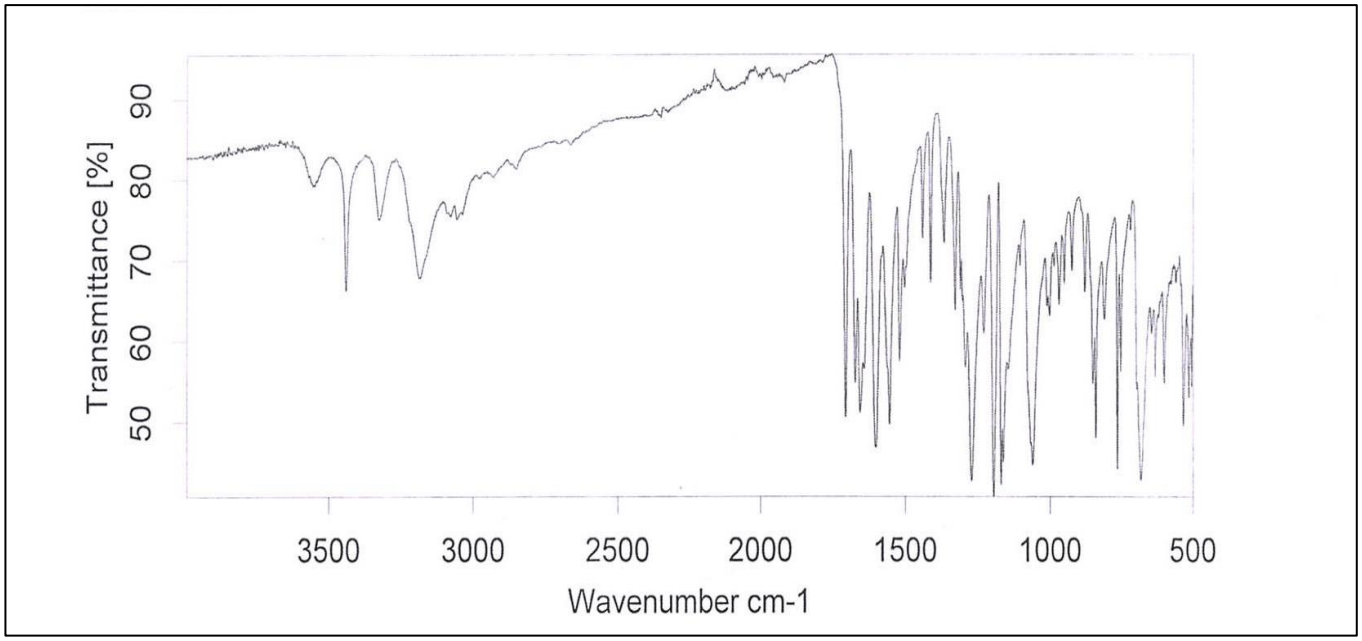

IR spectrum *(KBr)* ν_{max}/cm^{-1}***:*** 3323(-NH-), 3054, 2927, 1703 (-COO-), 1653, 1598 (-HC=N-), 1553, 1364, 1291,1270, 839.

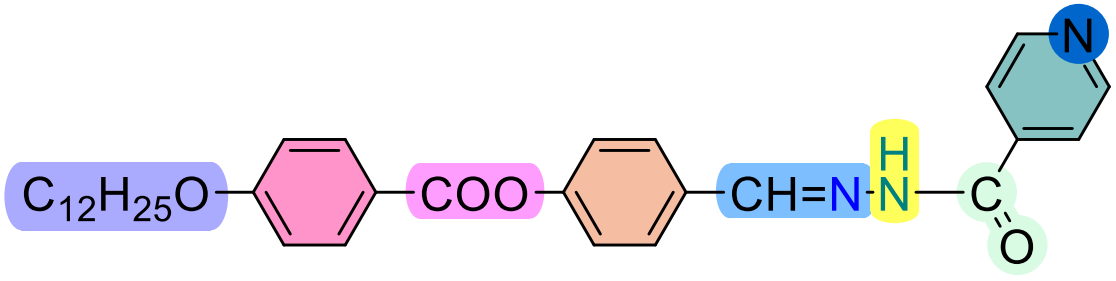

4-((2-isonicotinoylhydrazineylidene)methyl)phenyl 4-(dodecyloxy)benzoate

Journal of Chemical Health Risks
www.jchr.org
JCHR (2025) 15(6), 1753-1772 | ISSN:2251-6727

Figure:3 IR Graph

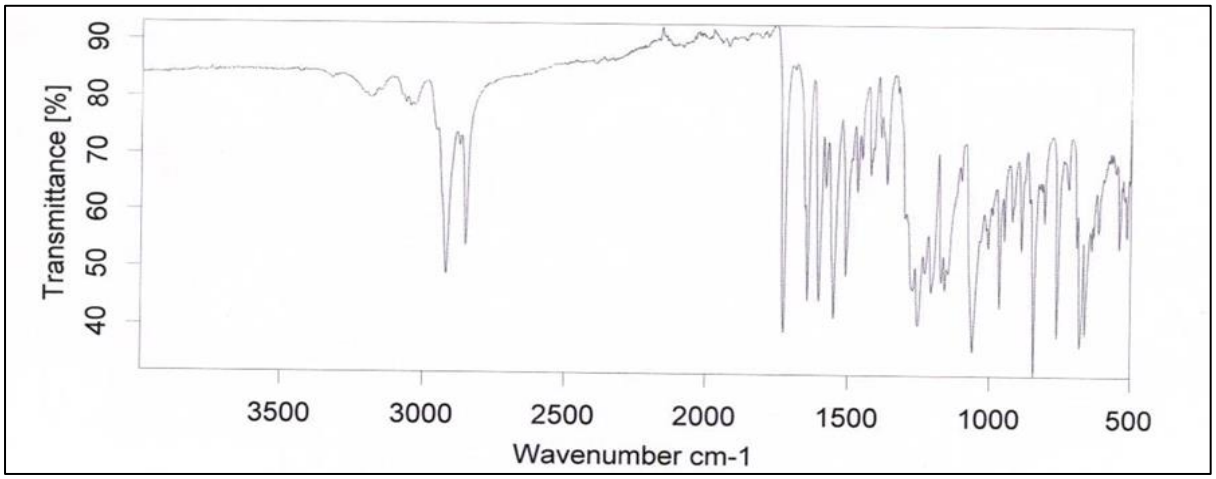

IR spectrum *(KBr)* ν_{max}/cm^{-1}**:** 3179 (-NH-), 1724 (-COO-), 1601 (-HC=N-), 1553, 1364, 1291,1270, 839.

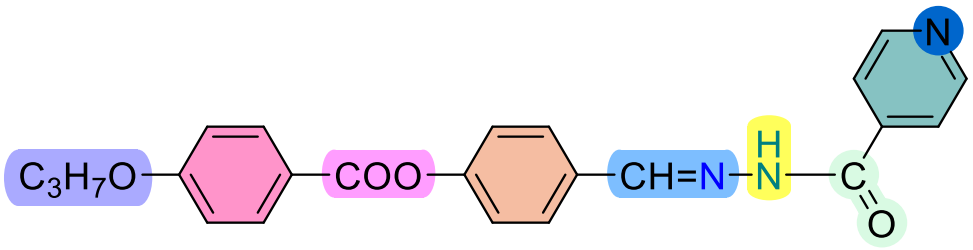

4-((2-isonicotinoylhydrazineylidene)methyl)phenyl 4-propoxybenzoate

Figure:4 NMR Graph

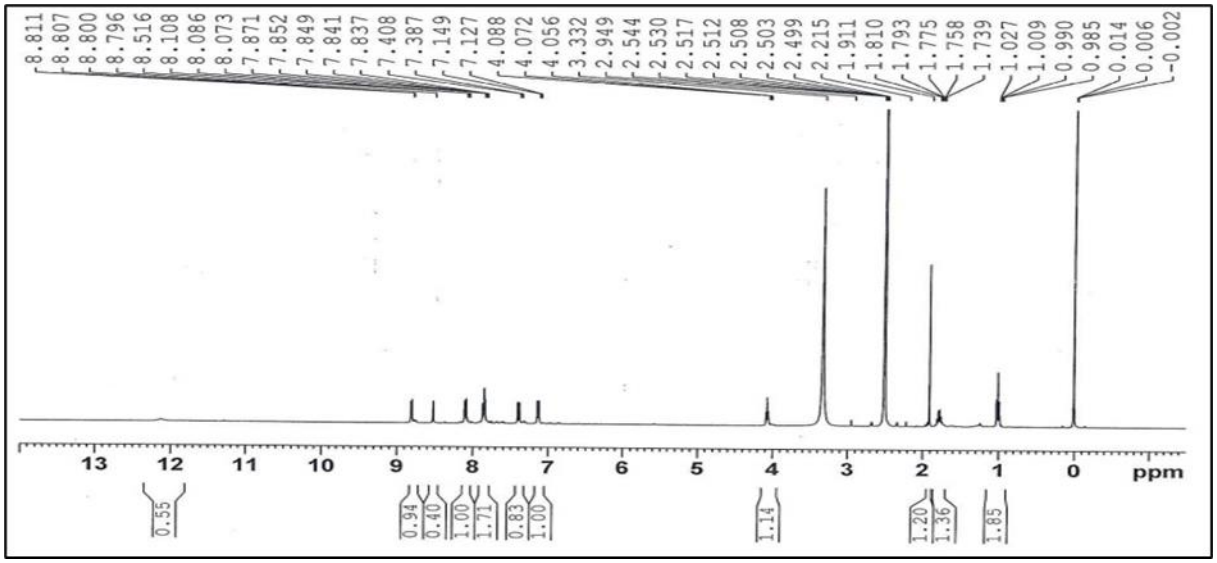

^{1}H NMR (500 MHz, $CDCl_3$) δ 11.57 (s, 1H), 7.12 (s, 1H), 8.81 – 8.07 (m, 2H), 8.07 – 8.00 (m, 2H), 7.96 – 7.40 (m, 4H), 7.38 – 7.14 (m,4H), 7.21 – 7.12 (m, 2H), 4.08 – 3.32 (m, 2H),) 1.09 – 1.02 (m, 2H), 0.99 (m, 3H)

Journal of Chemical Health Risks

www.jchr.org

JCHR (2025) 15(6), 1753-1772 | ISSN:2251-6727

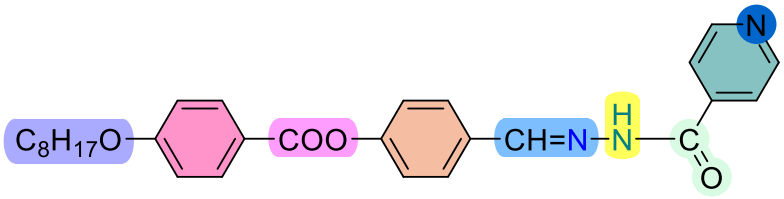

4-((2-isonicotinoylhydrazineylidene)methyl)phenyl 4-(octyloxy)benzoate

Figure:5 NMR Graph

^{1}H NMR (500 MHz, $CDCl_3$) δ 12.10 (s, 1H), 10.03 (s, 1H), 8.81 – 8.79 (m, 2H), 8.07 – 8.00 (m, 2H), 7.96 – 7.40 (m, 4H), 7.38 – 7.14 (m,4H), 7.21 – 7.12 (m, 2H), 4.11 – 4.08(m, 2H),) 2.95 – 1.24 (m, 12H), 0.858 (m, 3H)

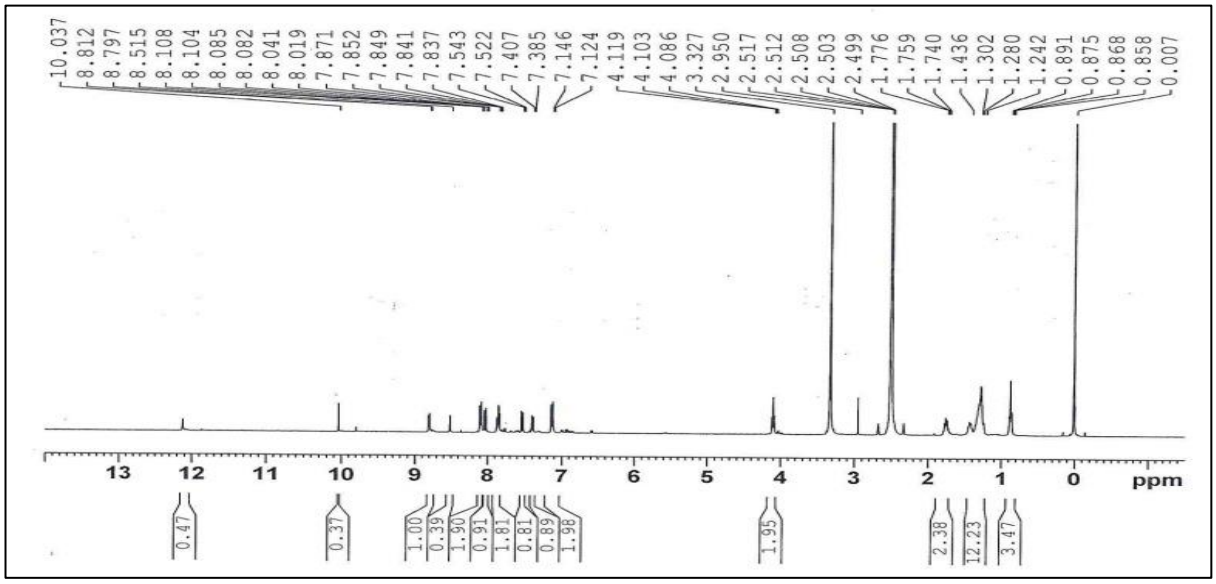

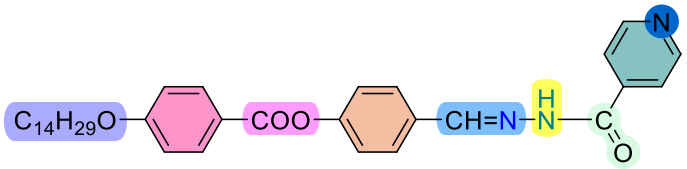

4-((2-isonicotinoylhydrazineylidene)methyl)phenyl 4-(tetradecyloxy)benzoate

Figure:6 NMR Graph

^{1}H NMR (500 MHz, $CDCl_3$) δ 12.11(s, 1H),8.81 (s, 1H), 8.81 – 8.79 (m, 2H), 8.78 – 8.51(m, 2H), 8.08 – 7.54 (m, 4H), 7.45 – 7.12 (m,4H), 7.21 – 7.12 (m, 2H), 4.11 – 4.08(m, 2H),) 2.51 – 1.03 (m, 24H), 0.86 (m, 3H)

Journal of Chemical Health Risks

www.jchr.org

JCHR (2025) 15(6), 1753-1772 | ISSN:2251-6727

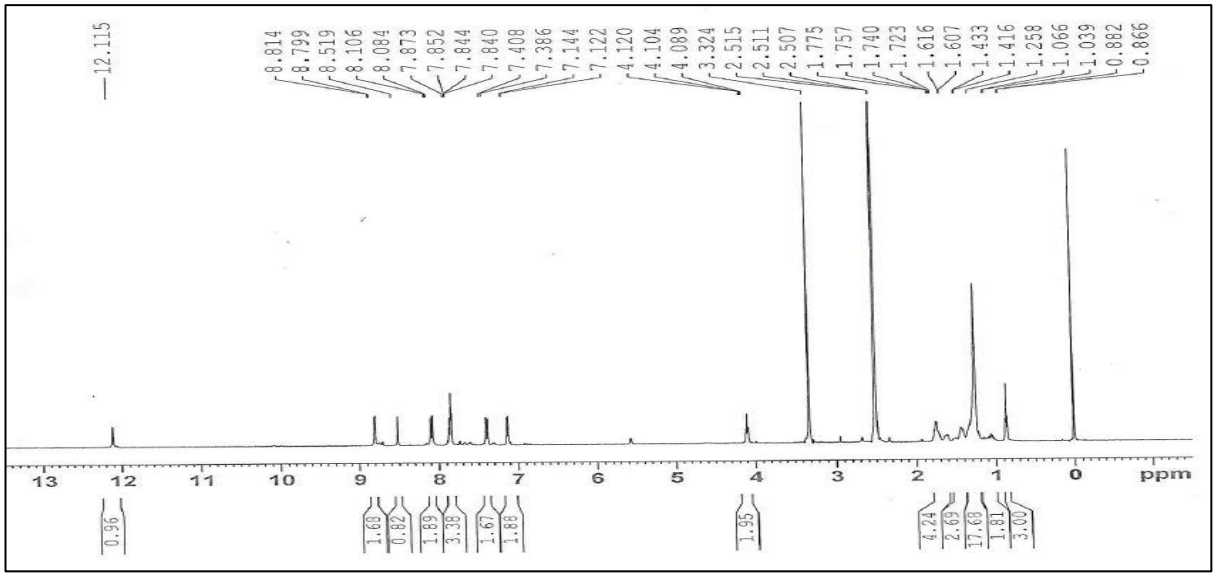

Result And Discussion

Optical microscopy studies

As a first step, the optical microscopic examinations were used to determine the mesophases that compounds of series **I** displayed. Isotropic liquids of series **I,** All the members exhibited enantiotropic schlieren nematic phase. *n*-methoxy to *n*-hexadecyloxy derivatives, exhibited enantiotropic nematic phase's characteristic schileren texture was formed by the derivatives [**Figure 14-17**] POM Study:

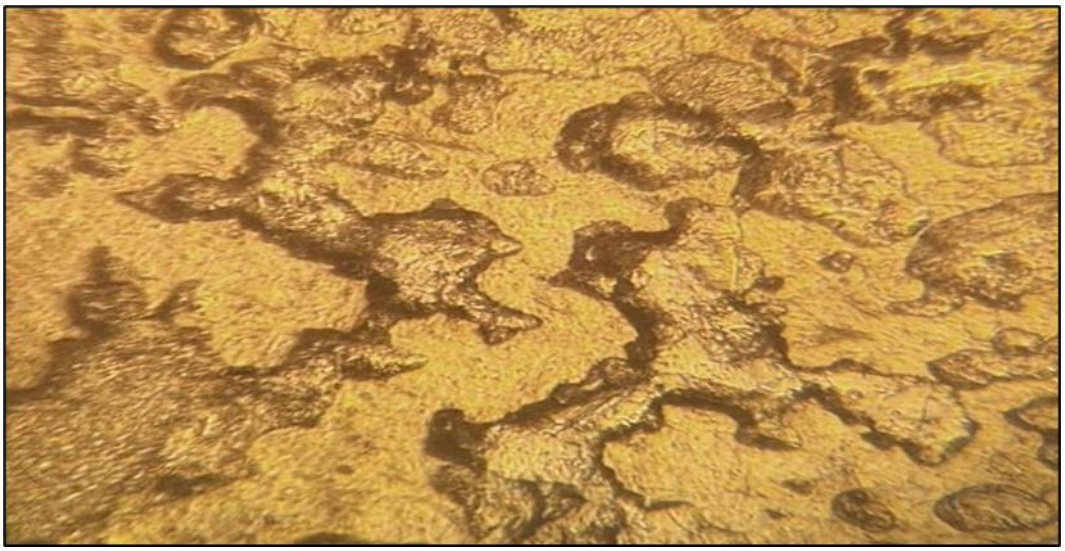

Figure 14. Microphotograph nematic mesophase (Series **I**; *n*=**4**) at **172 ºC** on cooling

Journal of Chemical Health Risks
www.jchr.org
JCHR (2025) 15(6), 1753-1772 | ISSN:2251-6727

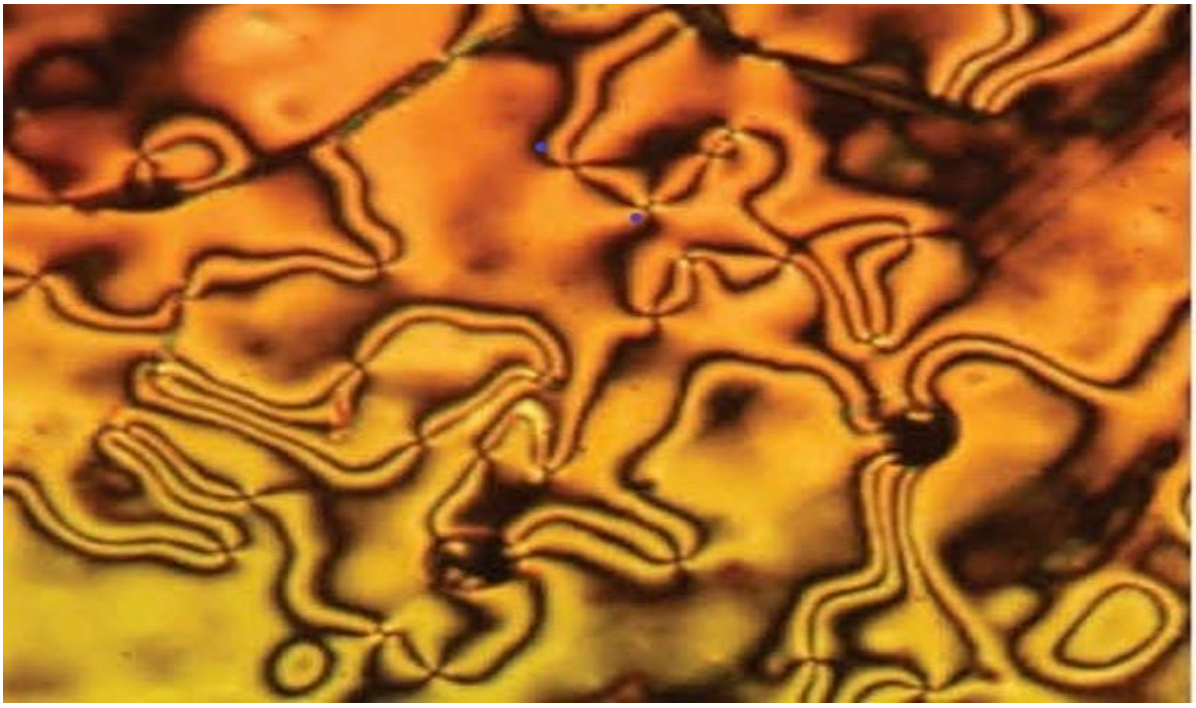

Figure 15. Microphotograph nematic mesophase (Series **I**; *n*=**8**) at **180 ºC** on cooling

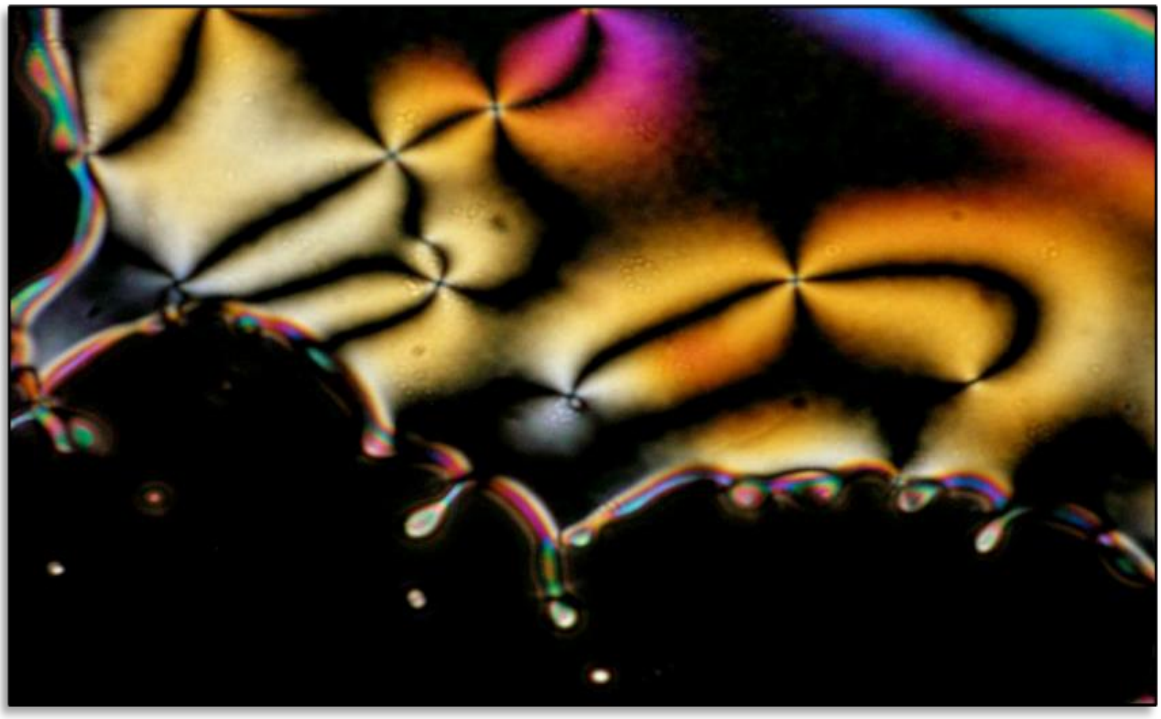

Figure 16. Microphotograph nematic mesophase (Series I; n=12) at 170 ºC on cooling

Journal of Chemical Health Risks
www.jchr.org
JCHR (2025) 15(6), 1753-1772 | ISSN:2251-6727

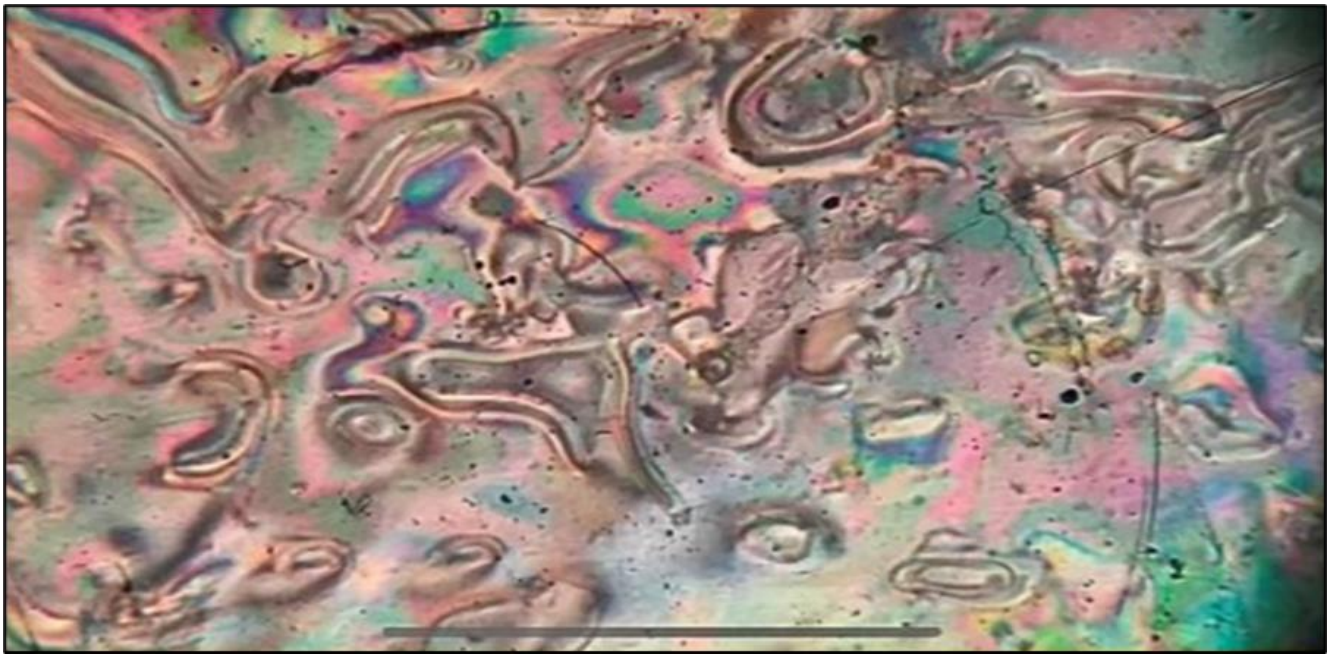

Figure 17. Microphotograph nematic mesophase (Series I; n=14) at 160 ºC on cooling

Table 1 contains information about the transition temperatures. **Figure 1-3** displays the IR graphs & ^{1}H NMR **Figure 4-6**

Calorimetric studies

Phase transitions can be detected with the use of calorimetry. We can make inferences about the characteristics of the phases that take place during the transitions since it produces quantifiable results. The enthalpies of derivative of series **I** (n = 1,3,4,5,8,12) and (n = 16) were determined in the current investigation using differential scanning calorimetry. The information is documented in **Table 3**. There are thermograms in [**Figures 7-13] DSC:**

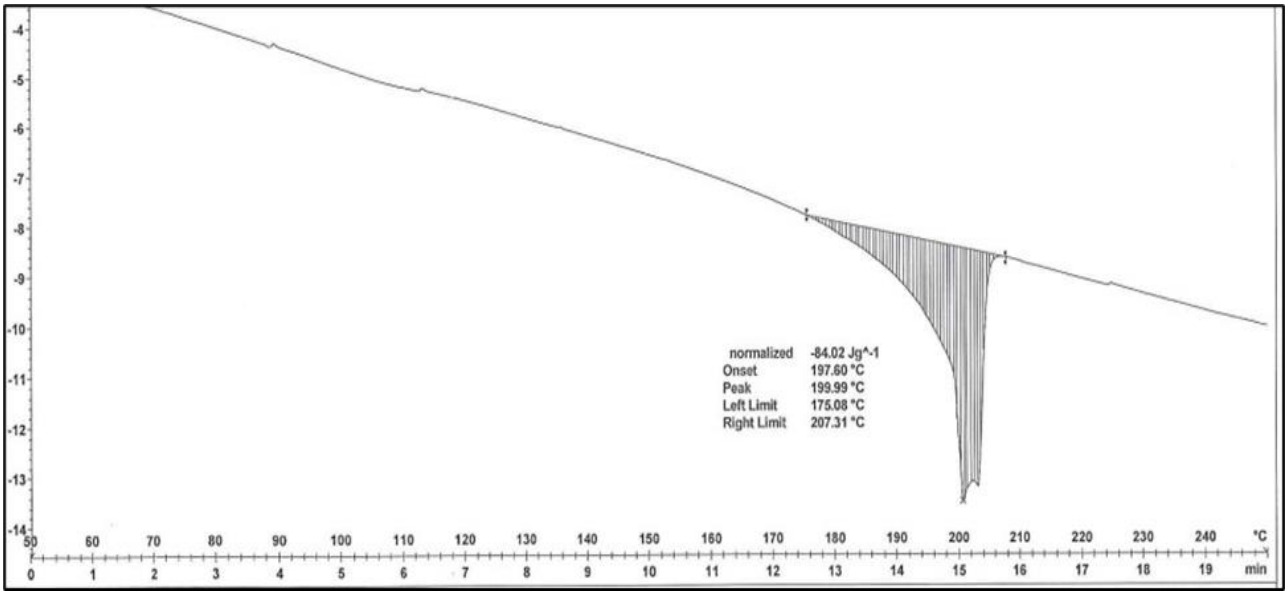

Figure: 7 DSC data - thermogram of compound 1

Journal of Chemical Health Risks
www.jchr.org
JCHR (2025) 15(6), 1753-1772 | ISSN:2251-6727

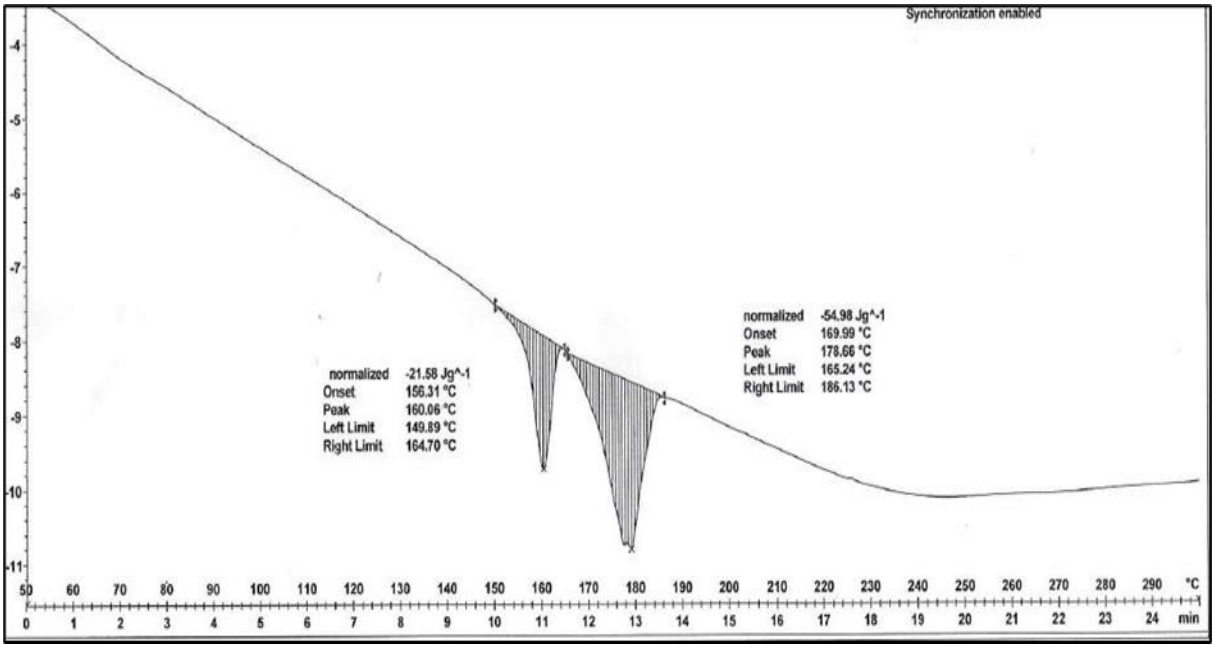

Figure: 8 DSC data - thermogram of compound 3

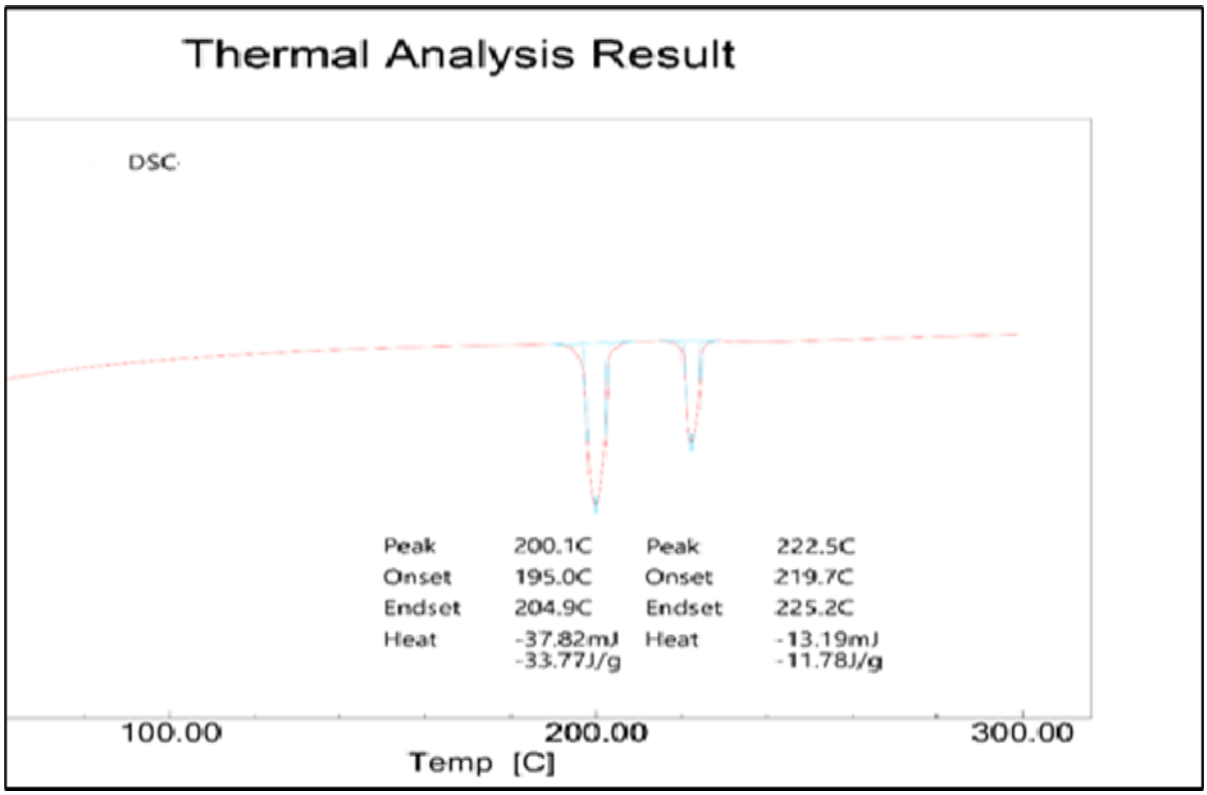

Figure: 9 DSC data - thermogram of compound 4

Journal of Chemical Health Risks
www.jchr.org
JCHR (2025) 15(6), 1753-1772 | ISSN:2251-6727

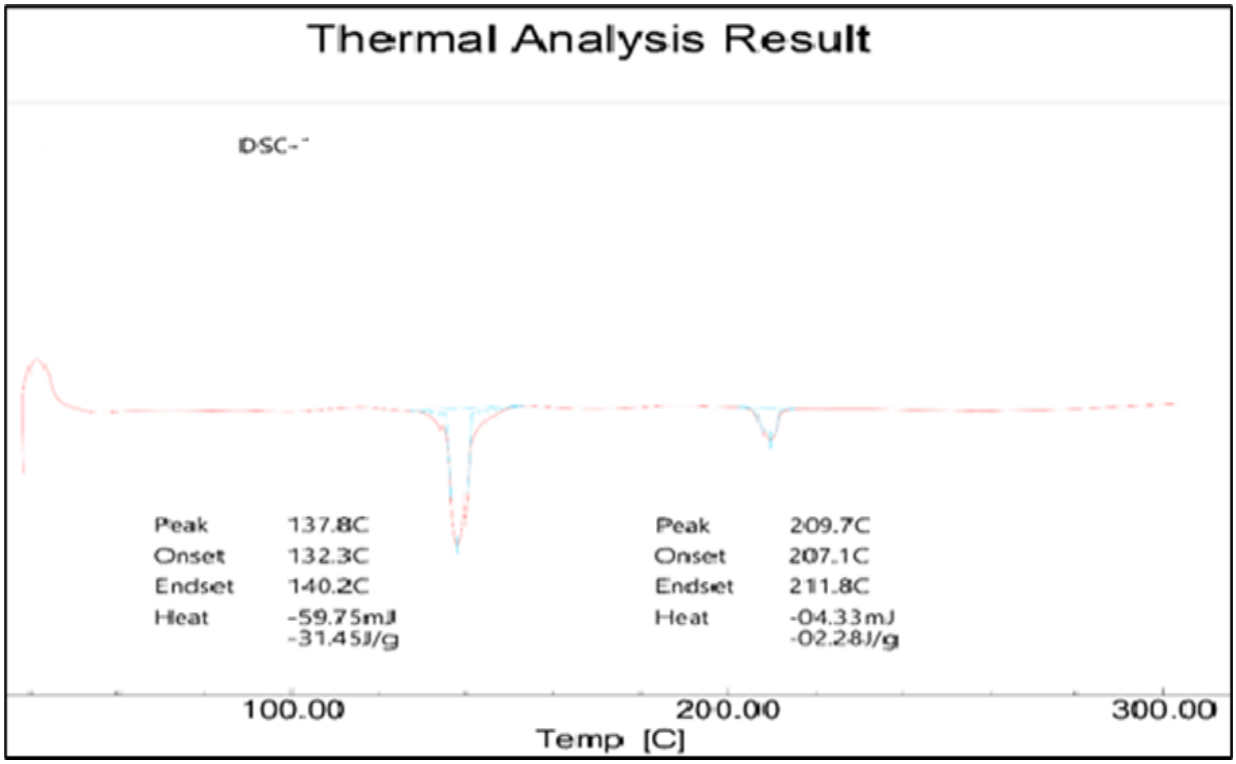

Figure: 10 DSC data - thermogram of compound 5

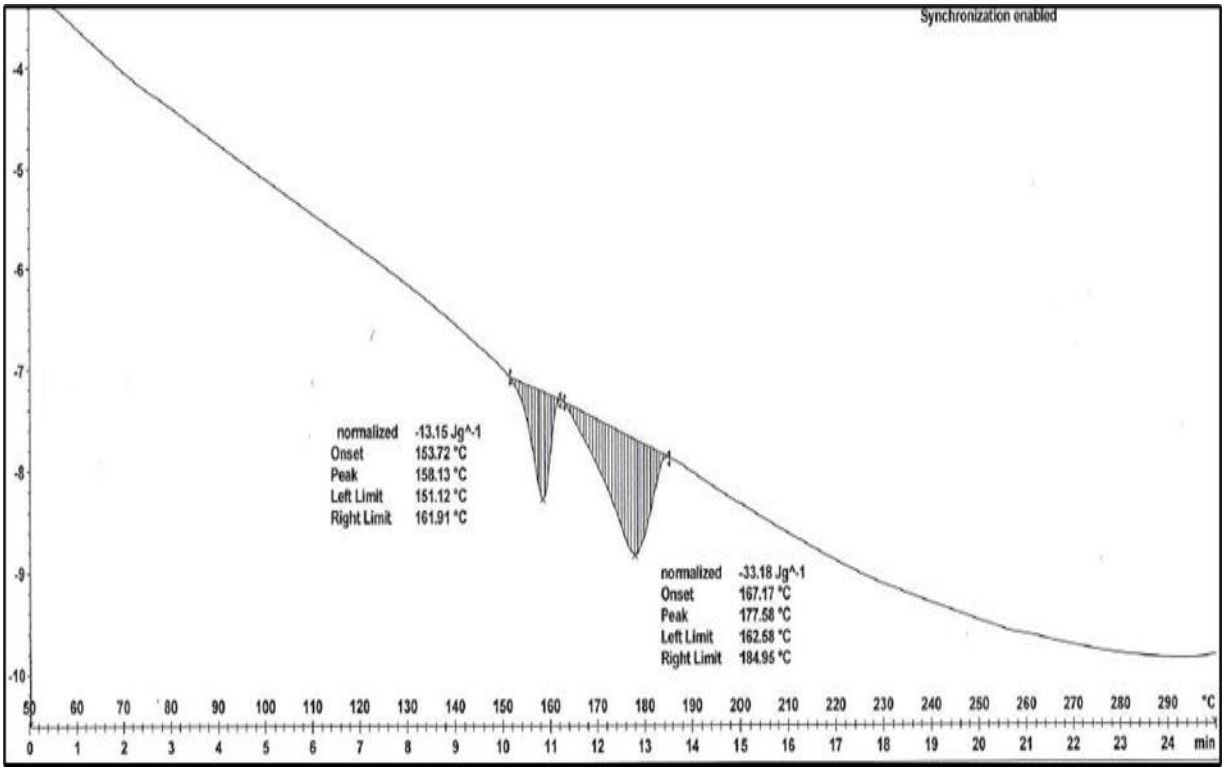

Figure: 11 DSC data - thermogram of compound 8

Journal of Chemical Health Risks

www.jchr.org

JCHR (2025) 15(6), 1753-1772 | ISSN:2251-6727

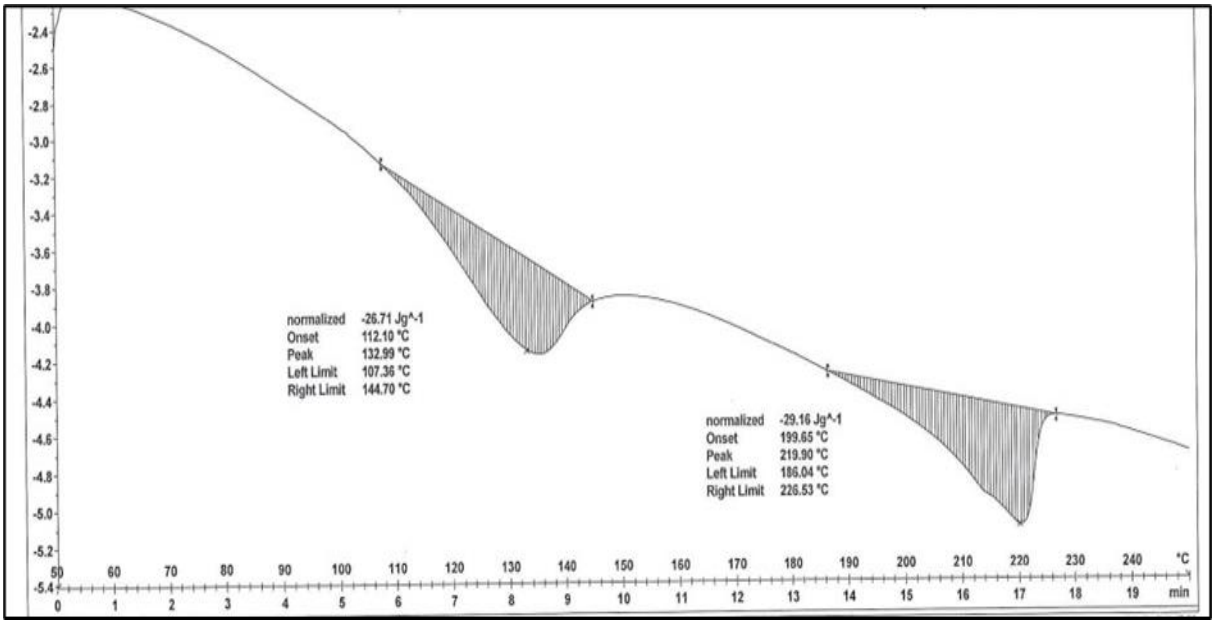

Figure: 12 DSC data - thermogram of compound 12

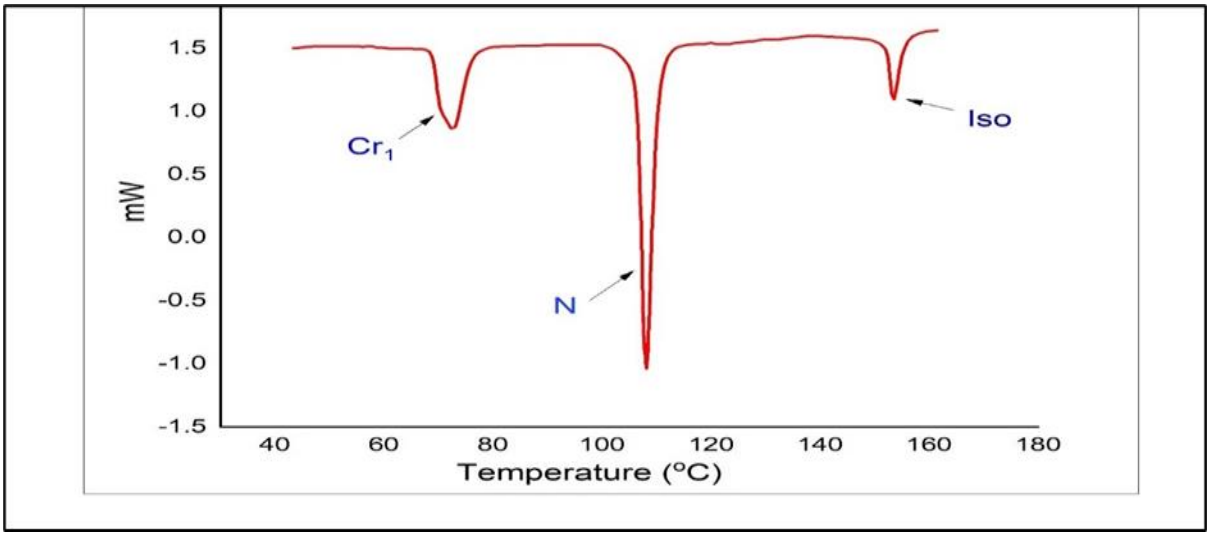

Figure: 13 DSC data - thermogram of compound 16

Docking Study:

To analyze the potency of these molecules various receptor proteins were selected for docking studies. Applying Schrödinger software, molecular research was performed to check the binding interaction between INH compounds (1 to 12, A to L, and A to K) and active sites of the receptor proteins. To perform preparations of proteins "protein preparation" module of Schrödinger software version 13.4 was used using default parameters. Then for ligand preparation "Ligprep" module was utilized with default setting. The receptor grid was also prepared with default setting. The ligands were molecularly docked to the receptor in the glide Extra precision (XP) mode using the default settings. These studies were done to know the effective binding interactions between the INH molecules and the receptor proteins. **[19-23] Figure [18] Docking, Table- [4-6]** indicates computational work.

Journal of Chemical Health Risks
www.jchr.org
JCHR (2025) 15(6), 1753-1772 | ISSN:2251-6727

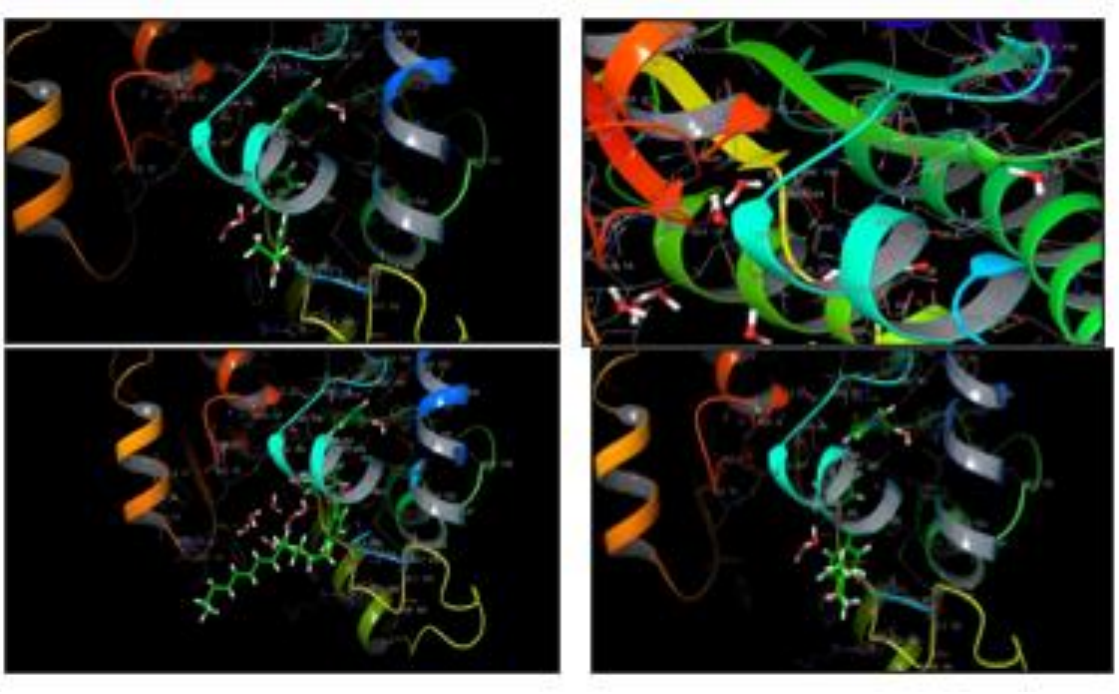

Figure 18 .3D interaction pose of VSBs with PDB ID: 4TZK, PDB ID: 2V2E and PDB ID: 3I6N

Comparing the nematic mesophase range, transition temperature, and molecular structure of representative compound **of series 1** (*n*=6) of the current series I*6* with structurally related other compounds **A [24]** is summarized in **Table 7**

The N-I transition temperature and nematic mesophase range of compound **I$_6$** are 70˚C and compound **A$_6$** 46˚C lower, correspondingly, than those of compound **A$_6$**. There is only one terminal where compound **I$_6$** molecular structure differs from compound **A**'s. Compound **I$_6$** contains a terminal **(-N-)** at the same end as compound **A$_6$**, while compound has an **(-H-)** connection. The length in addition to overall Ability of the rod-shaped molecules to be polarized are increased when added to the system, as indicated by Gray **[25]**.

Table:4 Docking score of INH Compounds

PDB: 4TZK Mycobacterium tuberculosis enoyl reductase

COMPOUND	**GLIDE SCORE**
INH COMP -1	-7.665
INH COMP -2	-7.249
INH COMP -3	-7.173
INH COMP -4	-7.108
INH COMP -5	-7.096
INH COMP -6	-6.795

Journal of Chemical Health Risks
www.jchr.org
JCHR (2025) 15(6), 1753-1772 | ISSN:2251-6727

INH COMP -7	-6.667
INH COMP -8	-6.454
INH COMP -9	-6.395
INH COMP -10	-6.306
INH COMP -11	-6.288
INH COMP -12	-6.222

Table:5 Docking score of INH Compounds

PDB: 2V2E Mycobacterium tuberculosis

COMPOUND	GLIDE SCORE
INH COMP -1	-8.282
INH COMP -2	-7.526
INH COMP -3	-7.271
INH COMP -4	-7.208
INH COMP -5	-6.504
INH COMP -6	-6.416
INH COMP -7	-5.790
INH COMP -8	-4.933
INH COMP -9	-4.306
INH COMP -10	- 4.125
INH COMP -11	-4.060
INH COMP -12	-3.411

Table:6 Docking score of INH Compounds

PDB: 3I6N Mycobacterium tuberculosis

Journal of Chemical Health Risks

www.jchr.org

JCHR (2025) 15(6), 1753-1772 | ISSN:2251-6727

COMPOUND	GLIDE SCORE
INH COMP -1	-4.146
INH COMP -2	-4.100
INH COMP -3	-3.590
INH COMP -4	-3.264
INH COMP -5	-3.144
INH COMP -6	-2.970
INH COMP -7	-2.866
INH COMP -8	-2.859
INH COMP -9	-2.466
INH COMP -10	-1.822
INH COMP -11	-1.595

Table-7 Comparison of the phase transition temperatures, nematic mesophase range and comparative molecular structures of compounds of Series I and Series A

Compound	Nematic range	Isotropic range	Mesophase range/ ˚C	Commencement of nematic phase
Series I	135	205	70	C_1
Series A	110.8	156.8	46	C_4

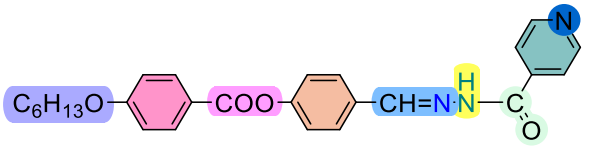

Series I

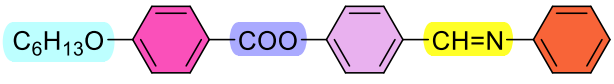

Series A

Conclusion:

The stability and development of mesophases were examined in a new family of Schiff base ester liquid crystal compounds, Alkyl 4-[(E)-{4-[(pyridin-4-ylcarbonyl) hydrazono] methyl} phenoxy] benzoates. The following was found by the study:

(1) It was discovered that all Schiff base group compounds, regardless of the length of the alkoxy chain or the polarity of the terminal substituent N, are mesomorphic with nematic phases; homologues are exclusively nematogenic.

(2) In comparison to the azo ester analogue, the Schiff base ester series exhibits high mesophase stability.

Journal of Chemical Health Risks

www.jchr.org

JCHR (2025) 15(6), 1753-1772 | ISSN:2251-6727

(3) N substituents' polarity and electrical interactions with the entire molecule have a greater impact on mesophase stability. It was discovered that the nematic range shrank for electron-releasing substituents N and expanded for electron-donating substituents N. This suggests that an additional factor of polarizability, which is crucial for stability and mesophase formation types, is provided by the increase in electron density on the ester linkage.

(4) The ligands were molecularly docked to the receptor in the glide Extra precision (XP) mode using the default settings. These studies were done to know the effective binding interactions between the INH molecules and the receptor proteins.

Declaration of conflict of Interest

The authors declare that they have no known competing financial interests or personal relationships that could have appeared to influence the work reported in this paper/publication.

Funding

The author(s) received no financial support for the research, authorship, and/or publication of this article.

Reference:

1. Adaway JE, Keevil BG, Owen LJ. Liquid chromatography tandem mass spectrometry in the clinical laboratory. Ann Clin Biochem. 2015;52(1):18-38.
2. Berchtold C, Bosilkovska M, Daali Y, Walder B, Zenobi R. Real-time monitoring of exhaled drugs by mass spectrometry. Mass Spectrom Rev. 2014;33(5):394-413.
3. Byrne FP, Jin S, Paggiola G, Petchey THM, Clark JH, Farmer TJ, et al. Tools and techniques for solvent selection: green solvent selection guides. Sustain Chem Process. 2016;4(7):1-24.
4. Chellini PR, Lages EB, Franco PHC, Nogueira FHA, Cesar IC, Pianetti GA. Development and validation of an HPLC method for simultaneous determination of rifampicin, isoniazid, pyrazinamide and ethambutol hydrochloride in pharmaceutical formulations. J AOAC Int. 2015;98(5):1234-9.
5. Ellard GA, Gammon PT, Wallace SM. The determination of isoniazid and its metabolites acetylisoniazid, monoacetylhydrazine, diacetylhydrazine, isonicotinic acid and isonicotinyl glycine in serum and urine. Biochem J. 1972;126(3):449-58.
6. Blagden N, de Matas M, Gavan PT, York P. Crystal engineering of active pharmaceutical ingredients to improve solubility and dissolution rates. Adv Drug Deliv Rev. 2007; 59:617-30.
7. Priya B, Johnson D, Dubey G, Suthar D, Kumar IP, Thiruvenkatam V, et al. Temozolomide cocrystal forms with enhanced dissolution, stability and biological activity towards glioblastoma. J Mol Struct. 2024; 1313:138751.
8. Hua XN, Pan X, Zhu Y, Cai ZE, Song Q, Li YZH, et al. Novel pharmaceutical salts of cephalexin with organic counterions: structural analysis and properties. RSC Adv. 2022;12:34843-50.
9. Berry DJ, Steed JW. Pharmaceutical cocrystals, salts and multicomponent systems: intermolecular interactions and property based design. Adv Drug Deliv Rev. 2017;117:3-24.
10. Lima GC, Silva EV, Magalhães PdO, Naves JS. Efficacy and safety of a four-drug fixed-dose combination regimen versus separate drugs for treatment of pulmonary tuberculosis: a systematic review and meta-analysis. Braz J Microbiol. 2017;48(2):198-207.
11. Wilkins CA, Hamman H, Hamman JH, Steenekamp JH. Fixed dose combination formulations in solid oral drug therapy: advantages, limitations, and design features. Pharmaceutics. 2024;16(2):178.
12. Subashini R. Oral delivery of ascorbic acid stabilized rifampicin nanoparticles for enhanced bioavailability of rifampicin [dissertation]. Tiruchengode: Swamy Vivekanandha College of Pharmacy; 2013.
13. Albanna AS, Smith BM, Cowan D, Menzies D. Fixed-dose combination antituberculosis therapy: a systematic review and meta-analysis. Eur Respir J. 2013;42(3):721-32.
14. Gray GW, Jones B. J Chem Soc. 1953:4179; 1954:678, 683, 1467; 1955:236.
15. Jones B. J Chem Soc. 1935:1874.
16. Dave JS, Vora RA. Liquid crystals and ordered fluids. In: Johonson JF, Porter RS, editors. New York: Plenum Press; 1970. p. 477.

17. Hassen A, Alexanian V. Tetrahedron Lett. 1978:4475.
18. Dave JS, Patel PR. Mol Cryst. 1966;2:115.
19. Jisha SP, Nagesh GY, Karunakar P, Nidhi G, Sridhar BT, Basavarajaiah SM. Exploration of novel isoniazid embedded 1,3,4-oxadiazole hybrids as anti-TB, antioxidant and COX inhibitors: synthesis, spectral analysis and molecular modeling studies. J Iran Chem Soc. 2025;22(4):717-31.
20. Verma R, Boshoff HI, Arora K, Bairy I, Tiwari M, Varadaraj BG, et al. Synthesis, evaluation, molecular docking and molecular dynamics studies of novel N-(4-[pyridin-2-yloxy]benzyl)arylamine derivatives as potential antitubercular agents. Drug Dev Res. 2020;81(3):315-28.
21. Shaikh SI, Zaheer ZAH, Mokale SN, Lokwani DK. Development of new pyrazole hybrids as antitubercular agents: synthesis, biological evaluation and molecular docking study. Int J Pharm Pharm Sci. 2017;9(11):50-6.
22. Thomas B, Harindran J. Design, synthesis and evaluation of antitubercular activity of Mannich bases of isoniazid-containing thiazolidin-4-one rings. Drug Discov. 2014;7: (pagination not available).
23. Suma KB, Kumari A, Shetty D, Fernandes E, Chethan DV, Jays J, et al. Structure-based pharmacophore modelling approach for the design of azaindole derivatives as DprE1 inhibitors for tuberculosis. J Mol Graph Model. 2020;101:107718.
24. Hagar M, Ahmed HA, Saad GR. Mesophase stability of new Schiff base ester liquid crystals with different polar substituents. Liq Cryst. 2018;45(9):1324-32.
25. Gray GW. Molecular structure and the properties of liquid crystals. London: Academic Press; 1962. p. 132147.